SINGLE CELL ANALYSIS OF IN VIVO HIV RESERVOIR UNCOVERS NOVEL MARKERS OF LATENT CELLS

Jason Neidleman[1,2], Xiaoyu Luo[2], Julie Frouard[1], Feng Hsiao[1], Guorui (Grace) Xie[1], Vincent Morcilla[3], Katherine Sholtis James[4], Rebecca Hoh[5], Ma Somsouk[6], Peter Hunt[7], Steve Deeks[5], Nancie Archin[4], Sarah Palmer[3], Warner C. Greene[2], Nadia R. Roan[1,2]

[1]Department of Urology, University of California, San Francisco, CA, [2]Gladstone Institute of Virology and Immunology, San Francisco, CA, [3]Centre for Virus Research, Westmead Institute for Medical Research, Sydney, Australia, [4]Department of Medicine, University of North Carolina, Chapel Hill, NC, [5]Division of HIV, Infectious Diseases and Global Medicine, University of California, San Francisco, CA, [6]Department of Medicine, University of California, San Francisco, CA, [7]Division of Experimental Medicine, University of California, San Francisco, CA

ABSTRACT

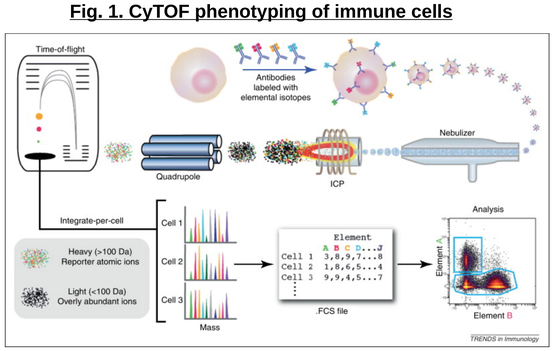
Background. Direct phenotypic analysis of the *in vivo* latent HIV reservoir is complicated by the need to reactivate these cells *ex vivo* to identify them, which changes the phenotypes of the latent cells. We used CyTOF to quantitate the levels of 43 different proteins on reactivated cells from ART-suppressed, HIV-infected individuals, and implemented a bioinformatics approach to trace each reactivated cell to its original latent state.

Methods. PBMCs (n=7), rectosigmoid biopsies (n=7), and lymph node aspirates (n=2) from treated individuals were phenotyped by CyTOF immediately after cell isolation, or stimulated with PMA/ionomycin or LRAs and then phenotyped. Reactivated cells were traced back to their original pre-stimulation state using the bioinformatics approach PP-SLIDE (Cavrois et al, Cell Reports 2017). Markers identified as preferentially expressed on latent cells were validated by sorting the cells and then conducting viral outgrowth assays and proviral sequencing.

Results. Latent cells were non-randomly distributed amongst memory CD4+ T cells. Markers preferentially expressed on latent cells included those that were shared between donors (PD1, CCR5, CD2, CD49d, Ox40) and donor-specific ones (CXCR5, TIGIT, CCR6, CD28, CD7). Markers differentially expressed between latent cells in blood vs. tissues, and between latent cells reactivatable by different stimulation methods, were identified. Analysis of longitudinal samples suggested the phenotype of latent cells is stable over time. Multiparameter sorting revealed that donor-shared surface markers identified by CyTOF markedly enriched for latent cells with replication-competent HIV: Tfh, already highly enriched for replication-competent HIV, was further enriched by 3 orders of magnitude using such markers. Viral sequencing analysis revealed the enriched cells to be largely clonally expanded.

Conclusions. We have validated CyTOF phenotyping of reactivated latent cells paired with bioinformatics analysis by PP-SLIDE as an effective way to chart the *in vivo* blood and tissue HIV latent reservoir. Our results demonstrate that 1) latent cells are not randomly distributed amongst memory CD4+ T cells, 2) the phenotypes of latent cells are stable over time, 3) LRAs can target different latent cells than PMA/ionomycin, 4) there are shared as well as donor-specific surface markers of latent cells, and 5) sorting of cells based on surface markers identified by CyTOF markedly enriches for clonally-expanded latent cells with replication-competent HIV.

Fig. 1. CyTOF phenotyping of immune cells



Bendall *et al* 2012

Fig. 1: CyTOF is a single-cell protein quantitation tool that, compared to conventional flow cytometry, is not limited by spectral overlap and therefore allows for more parameters to be simultaneously monitored. Cells labeled with metal-conjugated antibodies are injected into the nebulizer, become aerosolized, are reduced to single cell-containing droplets, and are directed to the ICP torch, where they are vaporized, atomized, and ionized in the plasma. The high pass optic removes the low-mass ions resulting in an ion cloud that enters the TOF mass analyzer. Ions are separated based on mass and accelerated to the detector, which measures the quantity of each isotope for each individual cell. Data can then be exported in an FCS format and analyzed.

Fig. 2. Classifying HIV-infected cells requires overcoming issue of HIV-induced remodeling

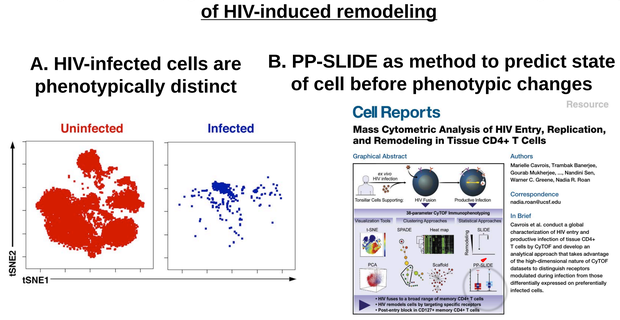


Fig. 2: (A) Uninfected and HIV-infected T cells isolated from tonsils of an uninfected donor were deep-phenotyped by CyTOF and analyzed by tSNE. The productively-infected cells (right) are largely phenotypically distinct from the uninfected T cells (left), as a result of remodeling of T cells by HIV. (B) A variety of high-dimensional analytical approaches can be used to visualize, quantitate, and account for viral-induced remodeling. One of these, PP-SLIDE, was developed as a single-cell high-dimensional analysis approach that predicts the phenotype of cells prior to cellular perturbations, in this case remodeling induced by HIV. Predictions made by PP-SLIDE were validated through cell sorting experiments. Adapted from Cavrois et al, 2017.

Fig. 3. *Ex vivo* reactivation to identify latent cells

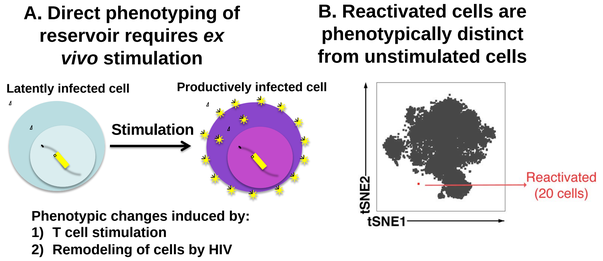


Fig. 3: (A) Direct phenotyping of the *in vivo* latent reservoir requires *ex vivo* stimulation in the presence of suppressive ART to reactivate the latent cells. Reactivation will induce phenotypic changes as a result of the *ex vivo* stimulation as well as remodeling of cells by HIV. (B) Visual demonstration by tSNE that reactivated cells from an HIV-infected individual are phenotypically distinct from unstimulated T cells from that individual.

Fig. 4. PP-SLIDE as a "molecular facial recognition" tool to predict the original state of changed cells

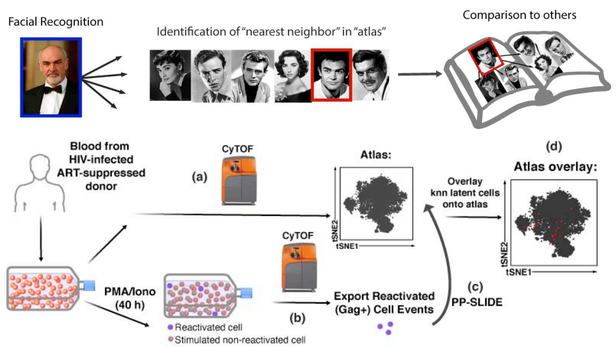


Fig. 4. *Top:* Facial Recognition analogy. *Bottom:* Schematic of use of PP-SLIDE to chart latent reservoir via CyTOF. CD4+ T cells from infected, ART-suppressed individuals were isolated and an aliquot immediately processed for CyTOF phenotyping *(a)*, while the remaining cells were treated with PMA/ionomycin for 40 hours in the presence of suppressive ART and then phenotyped *(b)*. PP-SLIDE was used to identify for every reactivated cell the corresponding knn latent cell (the phenotypically most similar cell in the atlas of unstimulated cells) *(c)*. An overlay of the knn latent cells (red) onto the atlas of unstimulated cells (grey) reveals regions preferentially associated with latency (*d*).

Fig. 5. Proof of Concept: PP-SLIDE identifies precursors of latent JLAT clones

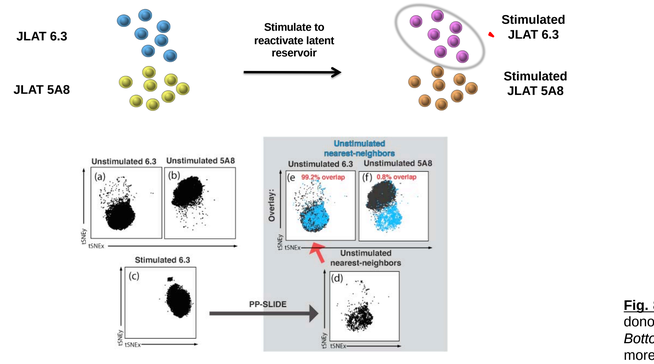


Fig. 5. Tracking activated JLAT cells to their parental clone by PP-SLIDE. *Top:* Experimental design. Unstimulated and PMA/ionomycin-stimulated JLAT clones 6.3 and 5A8 were deep-phenotyped by CyTOF, and PP-SLIDE was used to predict the precursor of stimulated 6.3. *Bottom:* t-SNE plots of unstimulated JLAT 6.3 (A), unstimulated JLAT 5A8 (B), and PMA/ionomycin-stimulated JLAT 6.3 (C). PP-SLIDE was used to identify the knn latent cell of each reactivated 6.3 cell in a merged file of unstimulated 6.3 and 5A8 cells. Note the marked overlap of the knn latent cells (D) with the unstimulated JLAT 6.3 (E, 99.2% overlap) and not JLAT 5A8 (F, 0.8% overlap), validating the ability of PP-SLIDE analysis of CyTOF-phenotyped cells to identify the pre-stimulation phenotype of reactivated latent cells.

Fig. 6. PP-SLIDE identifies precursors of reactivated cells from suppressed infected individuals

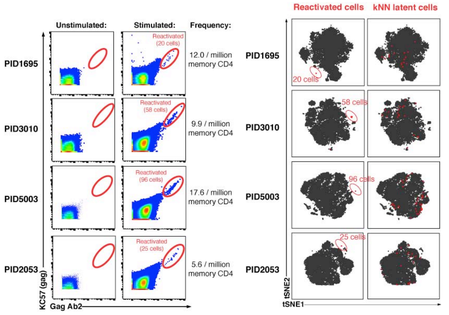


Fig. 6. *Left:* Identification of *ex vivo* reactivated latent cells from blood of infected ART-suppressed individuals. Cells were phenotyped prior or subsequent to stimulation for 40 hours with PMA/ionomycin in the presence of suppressive ART. Cells were stained for 3 different sets of anti-Gag antibodies. Shown are positive events as defined by dual staining for two of the anti-Gag antibodies. The frequencies of reactivated cells among memory CD4+ T cells is listed on the right. *Right:* The tSNE plots on the left show reactivated cells alongside unstimulated memory CD4+ T cells from the same patient. Due to phenotypic changes induced as a result of stimulation, the reactivated cells (stacked together as tight populations) reside in distinct regions of each tSNE plot. In the tSNE plots on the right, the reactivated cells were converted to their corresponding kNN latent cells by PP-SLIDE using all phenotyping parameters and visualized on the same tSNE atlas.

Fig. 7. Latent cells are non-randomly distributed

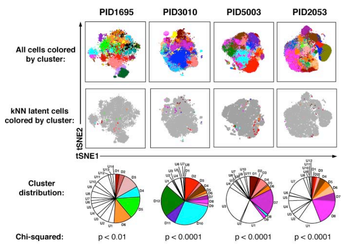


Fig. 7. kNN latent cells are non-randomly distributed among memory CD4+ T cells. The atlas of memory CD4+ T cells from each patient sample was clustered by FlowSOM. The tSNEs on the top present each cluster as a different color, while the tSNEs underneath show each kNN latent cell colored according to the cluster to which they belong. The pie graphs show the frequency of each of the clusters, with clusters harboring at least one kNN latent cell having a "D" designation (for "Detectable") and those lacking any kNN latent cells having an "U" designation (for "Undetectable"). The chi-squared values demonstrate the non-random distribution of the latent reservoir in all four patient samples.

Fig. 8. Different LRAs reactivate different latent cells

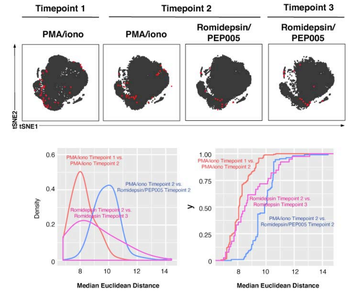


Fig. 8: *Top:* The atlas and kNN latent cells from three leukapheresis specimens from the same donor (PID5003), stimulated with either PMA/ionomycin or Romidepsin/PEP005 as indicated. *Bottom:* The kNN latent cells reactivatable by PMA/ionomycin at two different timepoints are more similar than between those reactivatable by PMA/ionomycin vs. Romidepsin/PEP005 at the same timepoint. The empirical cumulative distribution of median distances between kNN cells was calculated between 1) the Timepoint 1 PMA/ionomycin and Timepoint 2 PMA/ionomycin samples (red), and 2) the Timepoint 2 Romidepsin/PEP005 sample and Timepoint 3 Romidepsin/PEP005 samples (pink), and 3) the Timepoint 2 PMA/ionomycin and Timepoint 2 Romidepsin/PEP005 samples (blue). The density and probability plots are shown on the left and right sides, respectively.

Fig. 9. Features of the tissue reservoir

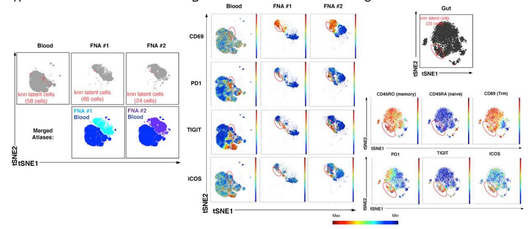


Fig. 9: A) The atlas of memory CD4+ T cells from fine needle aspirates (FNA) or leukapheresis blood specimens are depicted within the same t-SNE space. All three specimens were drawn from the same participant, and the two FNAs were drawn ~6 months apart. In the top set of plots, the atlas cells are shown in grey while the kNN latent cells are shown in red. In the bottom set of plots, each FNA atlas is overlaid with the blood atlas, demonstrating the minimal overlap of the blood and FNA cells on the tSNE. B) The tSNE maps presented in *panel A* are portrayed as heatmaps showing expression levels of the Trm marker CD69, and the indicated exhaustion/co-stimulatory molecules. C) F) *Top:* tSNE map showing the kNN latent cells from a gut specimen (red) overlaid onto the atlas of unstimulated CD4+ T cells (CD3+CD8-CD19-). *Bottom:* tSNE maps portrayed as heatmaps showing expression levels of the indicated antigen.

Fig. 10. PP-SLIDE provides method to markedly enrich for replication-competent, clonally expanded latent cells beyond PD1 selection

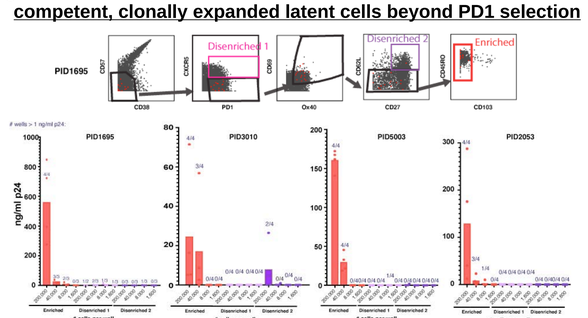


Fig. 10: Three different memory CD4+ populations all expressing high levels of PD1 were sorted from four HIV-infected, suppressed participants. Two are predicted to harbor low frequencies of latent cells (disenriched) while one is predicted to harbor high frequencies (enriched). Sorted cells were stimulated for 2 days with anti-CD3/CD28, diluted to the indicated number of cells per well, and cultured in the presence of MOLT-CCR5 cells for 15 days to allow for viral replication. Wells were then assayed by a p24 ELISA assay. A sample sort strategy for one of the donors is shown in the top panel. The results of the outgrowth assay are shown in the bottom panel. Viral outgrowth was scored two ways: the average concentration of p24 in each well per condition as depicted by the bar graphs, and the number of wells that had evidence of viral replication as depicted by the numbers above each bar (defined by a final p24 content of > 1 ng/ml). Viral sequencing by FLIPS reveals more intact p24 sequence in the Enriched population of PID1695 that has extensively clonally expanded (not shown).